Bacillus subtilis SecA ATPase Exists as an Antiparallel Dimer in Solution†

Haiyuan Ding,‡ John F. Hunt,§ Ishita Mukerji,‡ and Donald Oliver*,‡

Department of Molecular Biology and Biochemistry, Wesleyan University, Middletown, Connecticut 06459, and Department of Biological Sciences, Columbia University, New York, New York 10027

Received February 5, 2003; Revised Manuscript Received May 13, 2003

ABSTRACT: SecA ATPase promotes the biogenesis of membrane and secretory proteins into and across the cytoplasmic membrane of Eubacteria. SecA binds to translocon component SecYE and substrate proteins and undergoes ATP-dependent conformational cycles that are coupled to the stepwise translocation of proteins. Our recent crystal structure of *B. subtilis* SecA [Hunt, J. F., Weinkauf, S., Henry, L., Fak, J. J., McNicholas, P., Oliver, D. B., and Deisenhofer, J. (2002) *Science 297*, 2018−2026] showed two different dimer interactions in the lattice which both buried significant solvent-accessible surface area in their interface and could potentially be responsible for formation of the physiological dimer in solution. In this paper, we utilize fluorescence resonance energy transfer methodology with genetically engineered SecA proteins containing unique pairs of tryptophan and fluorophore-labeled cysteine residues to determine the oligomeric structure of SecA protein in solution. Our results show that of the two dimers interactions observed in the crystal structure, SecA forms an antiparallel dimer in solution that maximizes the buried solvent-accessible surface area and intermolecular contacts. At the submicromolar protein concentrations used in the fluorescence experiments, we saw no evidence for the formation of higher-order oligomers of SecA based on either the alternative dimer or the 3_1 helical fiber observed in the crystal lattice. Our studies are consistent with previous ones demonstrating the existence of a dimerization determinant within the C-domain of SecA as well as those documenting the interaction of N- and C-domains of SecA. Our results also provide a valuable starting point for a determination of whether the subunit status of SecA changes during the protein translocation as well as studies designed to elucidate the conformational dynamics of this multidomain protein during its translocation cycle.

The mechanism of protein translocation into and across the *Escherichia coli* plasma membrane has been the subject of intensive study given the relative biochemical simplicity and genetic tractability of this organism (see refs *1* and *2* for recent reviews). Targeting of membrane and presecretory proteins to the translocon typically utilizes the SRP−SRP receptor and SecA−SecB systems, respectively, although the basis for the division between these two pathways remains poorly defined (*3*−*7*). An additional component, YidC, is needed for the insertion of N-termini of integral membrane proteins (*8*, *9*). These pathways converge at the translocon, which consists of the core component SecYE and accessory proteins SecG and SecDF, which improve the efficiency of protein translocation, particularly at low temperatures. SecYE has been proposed to comprise the protein-conducting channel that has been visualized recently (*10*−*12*). SecA protein, the translocation ATPase, is central to the translocation process, since it interacts with both SecYE and the substrate protein and undergoes ATP-driven cycles of membrane insertion and retraction that are coupled to the stepwise translocation of proteins (see references contained in ref *1*). SecA membrane cycling may be enhanced by its coupling to cycles of SecG membrane topology inversion (*13*). SecDF has been proposed to enhance SecA-driven translocation by stabilizing SecA membrane insertion as well as by preventing back-sliding of the translocating polypeptide chain (*14*). However, SecDF is likely to perform an additional function in translocation, such as connecting YidC to SecYE (*15*), given its presence in Archaea that appear to lack a *secA* gene (*16*).

On the basis of the available genetic and biochemical evidence, a popular model for SecA-dependent protein translocation has been proposed which relies on ATP-driven cycles of SecA membrane insertion and retraction to drive translocation of successive segments of the substrate protein through the translocon (*17*, *18*). However, other models have been suggested as well. For example, the necessity of SecA membrane cycling has been questioned on the basis of the observation that active protein translocation occurred from SecA that was permanently embedded in the plasma membrane and which did not appear to undergo membrane cycling (*19*).

At physiological salt concentrations the SecA protein from *E. coli* forms a dimer in solution (*20*, *21*) that has been observed to form higher-order oligomers at elevated protein concentration (*21*, *22*) or to dissociate into monomers at elevated salt concentrations (*21*). Careful hydrodynamic studies have suggested that the structural properties of this

† This work was supported by Grants GM42033 and GM58549 from the National Institutes of Health to D.O. and J.H., respectively, and the Patrick and Catherine Weldon Donaghue Medical Research Foundation (DF#00-118) and the National Science Foundation (MCB-9507241) to I. M.

* Corresponding author. Phone: 860-685-3556. Fax: 860-685-2141. E-mail: doliver@wesleyan.edu.

‡ Wesleyan University.

§ Columbia University.

10.1021/bi0342057 CCC: $25.00
Published on Web 07/04/2003

dimer might change under certain solution conditions (*21*). Furthermore, the recently reported crystal structure of SecA from *Myobacterium tuberculosis* and associated studies indicate that the protein from that organism forms a tetramer under physiological conditions (*23*). Therefore, there is evidence for complexity in the oligomeric properties of SecA protein in aqueous solutions.

Moreover, there is controversy concerning the oligomeric state of SecA during active protein translocation. Although it was originally reported that SecA was active as a dimer (*24*), it has been argued recently that SecA is active as a monomer. SecA interaction with anionic phospholipids was found to induce its monomerization, and a monomeric mutant SecA protein displayed some residual in vitro protein translocation activity (*25*). However, another report demonstrated that interaction of SecA protein with signal peptides under such conditions was sufficient to restore dimer formation but potentially using a different protein−protein interface (*26*). In this context, it is important to develop techniques that enable the oligomeric state and structure of SecA to be monitored in solution.

We recently reported the crystal structure of the SecA (Div) protein from *Bacillus subtilis* (*27*), which is highly homologous to its *E. coli* homologue (*28*, *29*). While these crystals formed in the presence of very high salt (∼2 M ammonium sulfate), the protein concentration present in the crystallization reactions was also very high (∼0.2 mM) so that the physiological dimer structure was assumed to be retained in the crystal lattice despite the reduction in the affinity constant for dimerization observed under high-salt conditions (*21*). Although the asymmetric unit in these crystals contained a single SecA protomer, the symmetry of the lattice resulted in two interprotomer interactions characterized by proper 2-fold rotational symmetry, giving two potential candidates for the structure of the physiological dimer of SecA (*20*, *21*). Because one of these potential dimers buried a larger area of solvent-accessible protein surface in its interface (2800 vs 900 Å^2), it was designated as the "likely physiological dimer" in our previous paper (referred to here as the antiparallel dimer) (*27*). However, the molecular characteristics of packing contacts in protein crystals are quite complex (*30*−*37*). While nonphysiological crystal packing contacts have been observed on occasion that bury on the order of 2000 Å^2 (*38*−*40*), 900 Å^2 is still relatively high compared to the typical crystal packing contact (*30*−*33*).

Furthermore, in the case of the SecA crystals, an additional high-order protein interaction was observed in the lattice, involving the formation of a 3_1 helical fiber that buries 1900 Å^2 at the interface of two antiparallel dimers. An oligomer of this type could potentially have a tendency to form in solution based on the observation that SecA transiently forms higher-order oligomers at high protein concentrations (*20*−*22*) and stably forms higher-order oligomers in the presence of signal peptides at physiological temperature (*26*). Given these complexities, we set out to develop an experimental strategy to critically examine the structure of the SecA oligomer in solution. A technique that allows evaluation of the tendency of such higher-order structures to form in solution, in addition to providing information on the geometry of the physiological dimer, would be particularly useful.

Fluorescence resonance energy transfer (FRET) is a technique that has been widely applied to measuring intersite distances in macromolecules with suitably engineered fluorophores (*41*−*44*). In previous studies, FRET has been used effectively to establish the geometry of numerous macromolecular complexes, including protein−nucleic acid complexes (*45*) and multiprotein complexes (*46*, *47*). Depending on the donor−acceptor pair chosen for the experiment, distances up to 100 Å can be determined reliably. Common donor−acceptor strategies for proteins include the use of an intrinsic natural fluorophore, usually Trp, and an extrinsic label, introduced through covalent attachment to a Cys residue. This approach has been used recently to successfully examine conformational changes in troponin (*48*) and T4 DNA polymerase (*49*). While the accuracy of these distance measurements is limited to an extent by the uncertainly in the location and mobility of the extrinsic label covalently attached to the protein, suitably chosen donor−acceptor pairs have allowed distances between 20 and 100 Å to be determined with sufficient accuracy to allow reliable inferences to be drawn concerning both the details of protein conformational changes (*42*−*44*) and the structure of oligomeric complexes (*45*−*47*).

The FRET measurements performed in the present communication give experimental estimates of the distances between unique pairs of Trp and fluorophore-labeled Cys residues that were genetically engineered into SecA protein. The interresidue distances inferred from these measurements match those of one of the dimers observed in the crystal structure of *B. subtilis* SecA and thereby establish the structure of the SecA dimer in solution. In addition to enabling the nature of the subunit−subunit interactions between SecA to be monitored during its conformational reaction cycle, this system can also be applied to elucidating the nature of the conformational changes that occur within the SecA protomer during the ATP-driven protein translocation reaction, a goal that is central to understanding the mechanistic details of SecA-dependent protein translocation.

EXPERIMENTAL PROCEDURES

Chemicals. MIANS[1] and tris(2-carboxyethyl)phosphine hydrochloride were purchased from Molecular Probes (Eugene, OR). SP-Sepharose, hexyl agarose, β-mercaptoethanol, and most other reagent quality chemicals were from Sigma.

Mutagenesis. Substitution mutagenesis was performed on plasmid pT7div (*50*) or its derivatives by utilizing appropriate oligonucleotide primers and a Quik-Change site-directed mutagenesis kit (Stratagene) as described by the manufacturer. pT7div-W652 and pT7div-W724 have Trp724 and Trp652, respectively, substituted with Phe. pT7div-C4 was constructed by substitution of Cys825, Cys827, and Cys836 with Ser and Cys837 with His. Starting with pT7-C4 as template, the relevant mono-Trp mono-Cys derivatives used in this study were constructed. All mutations were confirmed by DNA sequence analysis. Plasmids were transformed into BL21.19 [*secA13(Am) supF(Ts) trp(Am) zch::Tn10 clpA::kan recA::cat*] (*51*) for SecA protein overproduction.

[1] Abbreviations: Div, *B. subtilis* SecA protein; FRET, fluorescence resonance energy transfer; IMV, inverted membrane vesicles; MIANS, 2-(4′-maleimidylanilino)naphthalene-6-sulfonic acid.

SecA, IMV, and Preprotein Preparation. SecA proteins were overproduced and purified essentially as described previously (*22*) with the following modification: SP-Sepharose and hexyl agarose chromatograpy was used instead of Mono-S and phenyl superose chromatography, respectively. Protein concentration was determined using the Bradford assay (BioRad) with bovine serum albumin as a standard. SecA ATPase activities were determined by the malachite green method (*52*) utilizing the modifications described previously (*51*). Wild-type IMV and IMV containing over-produced *B. subtilis* SecYEG protein were prepared from *E. coli* SF100 (*recA* Δ*lac* Δ*ompT*) and SF100 (pET822), respectively, as described previously (*53*). IMV were pretreated with 6 M urea in order to inactivate SecA protein as described previously (*54*). The chimeric preprotein PSN comprised of the *E. coli* alkaline phosphatase signal sequence and mature portion of Staphylococcal nuclease with K97C and W140H substitutions was prepared as described previously (*55*).

MIANS Labeling. SecA (0.3 mg/ml) in TKE buffer (25 mM Tris-HCl, pH 7.5, 25 mM KCl, 1 mM EDTA) was incubated on ice for 0.5−1 h with 30 μM tris(2-carboxyethyl)phosphine hydrochloride when a 4-fold molar excess of MIANS was added and the mixture was incubated on ice in the dark for an additional 3−4 h. The reaction was quenched by addition of a 10-fold molar excess of β-mercaptoethanol. The mixture was applied to a G-25 Sephadex column PD-10 (Pharmacia), and the void volume was collected in order to remove any free or β-mercaptoethanol-reacted MIANS. The SecA labeling efficiency was calculated as follows: the MAINS concentration of the protein adduct was determined from its absorbance at 324 nm using the molar extinction coefficient of MIANS ($\epsilon_{324\ nm} = 27000\ M^{-1}\ cm^{-1}$), while the SecA concentration was determined by the Bradford assay (BioRad) with bovine serum albumin as standard. The labeling efficiency was expressed as the molar ratio of MIANS to SecA monomer × 100%. The labeling efficiency was found to be 90−100% for nearly all of the mutant SecA proteins.

Fluorescence Measurements. Steady-state fluorescence spectra were recorded on a FluoroMax-2 spectrofluorometer (Instruments S. A., Metuchen, NJ) with a Neslab programmable water bath with a remote sensor. Sample was placed in a quartz cuvette with a 0.3 cm excitation and 0.3 cm emission path length. The excitation and emission slits were set at 0.94 mm to give a 4 nm band-pass. Spectra were scanned at a rate of 1 nm/s. Two or more data sets were collected for all experiments.

FRET Calculation. All the spectra were corrected for background. The efficiency of FRET (E) was calculated using the following equations (*41*):

$$E = (1 - F_{DA}/F_D)/f_a \quad (1)$$

where F_{DA} and F_D are the Trp fluorescence of SecA in the presence and absence of MIANS labeling, respectively, and f_a is the fraction of labeling. The efficiency of energy transfer is related to R_0, the Förster distance, and R, the distance between donor and acceptor, by the equation

$$E = R_0^6/(R_0^6 + R^6) \quad (2)$$

R_0 represents the distance where the transfer is 50% efficient and is calculated (in angstroms) as follows:

$$R_0 = 0.211[n^{-4} Q_D \kappa^2 J(\lambda)]^{1/6} \quad (3)$$

In the above equation, n is the refractive index (taken as 1.4), κ is the orientation factor (κ^2 was assumed to be 2/3 for a randomly oriented, mobile donor and acceptor pair), and Q_D is the quantum yield of the donor in the absence of acceptor. The quantum yields of Div-W652 and Div-W724 were measured relative to L-tryptophan and calculated to be 0.07 and 0.17 respectively, using the quantum yield of L-tryptophan as 0.13 (56). $J(\lambda)$, the overlap integral between donor emission and acceptor absorption, is calculated from the spectral data by

$$J(\lambda) = \int [\epsilon_A(\lambda)\lambda^4] f_D(\lambda)\, d\lambda \quad (4)$$

where $\epsilon_A(\lambda)$ is the molar extinction coefficient for acceptor ($M^{-1}cm^{-1}$) and f_D is the fluorescence intensity of the donor at wavelength λ (nm). The calculated Förster distance for MIANS-SH and Div-W652 or Div-W724 was 24.2 ± 0.3 or 27.8 ± 0.2 Å, respectively. The difference in Förster distance results from differences in both the overlap integral and quantum yield.

RESULTS

Construction and Characterization of SecA Proteins with Single Trp and Cys Residues. To differentiate between the potential SecA oligomers, a FRET analysis was performed on genetically engineered Div proteins containing unique Trp−Cys pairs. The pairs were chosen by measurements from the relevant structure (*27*) such that only one of the interprotomer distances of either the antiparallel or alternative dimers was capable of efficient energy transfer and there would be little contribution from intra-protomer FRET (Figure 1). Because FRET efficiency falls off with the inverse of the 6th power of the interfluorophore distance (eq 2 above), the site pair with the highest transfer efficiency within the distance range of $2R_0$ will dominate the FRET. Site pairs at distances $>2R_0$ are not expected to exhibit any energy transfer. Therefore, the distances inferred from FRET measurements will generally give the separation between the closest fluorophore pair in an ensemble. In addition, two Trp−Cys pairs (Trp652−Cys282 and Trp724−Cys282) were also chosen as controls so that their FRET efficiency would be dominated by intra-protomer energy transfer in order to serve as an internal standard to experimentally verify our methodology.

Div naturally contains only two Trp residues at positions 652 and 724 that correspond to Trp701 and Trp775 of *E. coli* SecA, respectively (*28*, *29*). Both of these residues are located within the C-terminal third of SecA, where Trp724 is buried within the α-helical scaffold domain, while Trp652 is located close to the surface of the α-helical wing domain (Figure 1A). Utilizing genetic engineering methodology where Trp was substituted with Phe, we constructed SecA protein derivatives that contain single Trp residues (see Experimental Procedures for details). Div-W652 and Div-W724 contain only Trp652 and Trp724, respectively. The fluorescence spectra of these proteins was examined utilizing an excitation wavelength of 297 nm where both Phe and

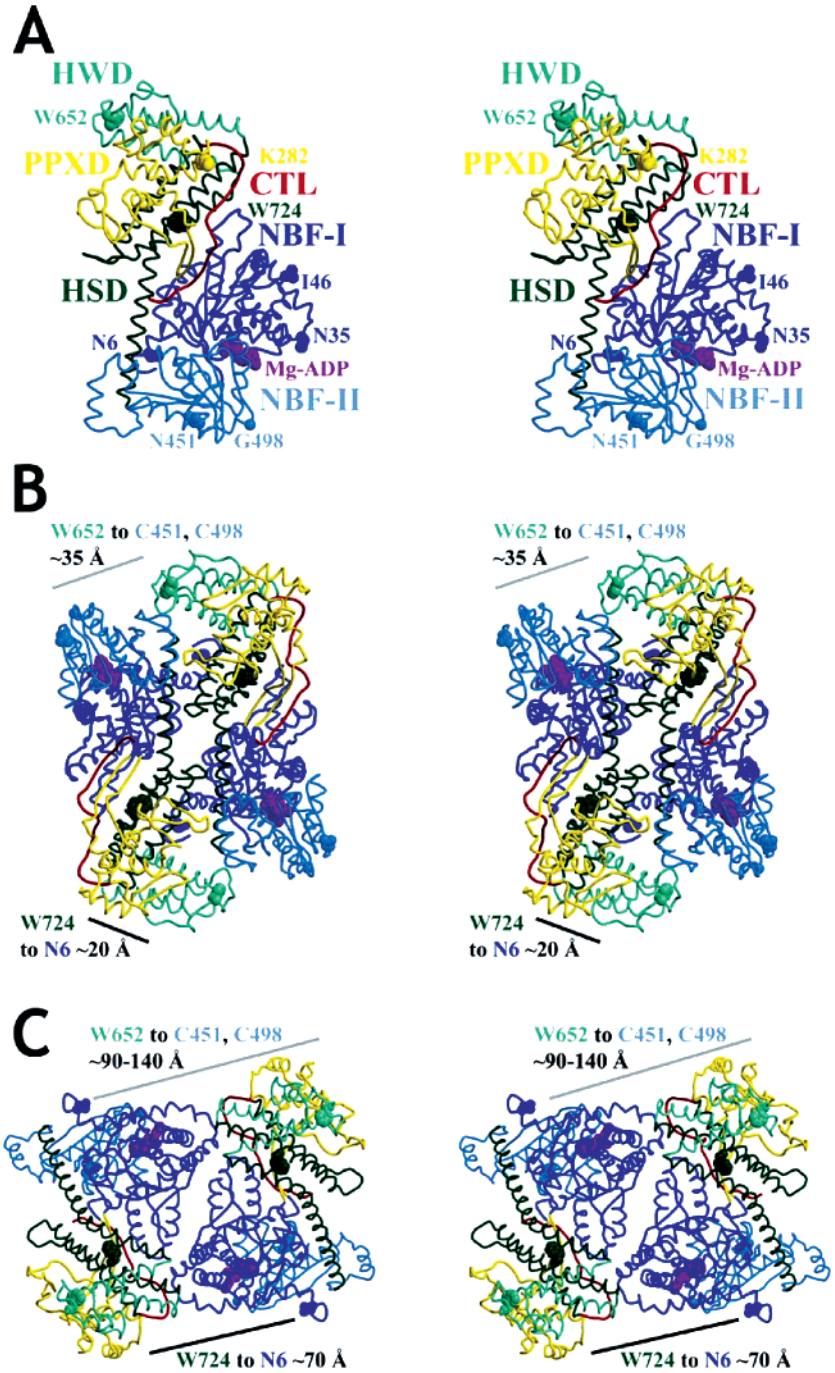

FIGURE 1: FRET sites in the crystallographic dimers of *B. subtilis* SecA. Stereo ribbon diagrams (74,75) of the *B. subtilis* SecA crystal structure are shown color-coded according to domain organization (27). The first nucleotide-binding fold (NBF-I) is shown in dark blue, the second nucleotide-binding fold (NBF-II) in cyan, the preprotein cross-linking domain (PPXD) in yellow, the α-helical scaffold domain (HSD) in dark green, the α-helical wing domain (HWD) in light green, and the C-terminal linker (CTL) in red. The Mg-ADP molecule bound to the high-affinity ATPase site is shown in a magenta space-filling representation. The side-chains of the residues at the sites used for the FRET experiments are shown in space-filling representations, colored according to the domain in which they are located. (A) View of the protomer showing the side chains at all of the sites employed in this study. (B, C) Views of the two crystallographic dimers (27) showing the side chains at the sites that allow for the different dimer models to be distinguished. The gray lines give an approximate indication of the separation between Trp652 in the HWD and the two cysteine sites (Cys451 and Cys498) in NBF-II, while the black lines give an approximate indication of the separation between Trp724 in the HSD and Cys6 in NBF-I. The dimer burying more solvent accessible surface-area in its interface, designated here as the antiparallel dimer, is shown in panel B, while the alternative dimer is shown in panel C. The first of these was identified as the likely physiological dimer by Hunt et al. (27).

Tyr residues have little absorption, and energy transfer between multiple tryptophan groups is minimized by excitation at the red edge of the adsorption spectrum (*57*). Div had a fluorescence peak at 333 nm, while Div-W652 and Div-W724 had fluorescence peaks at 339 and 330 nm, respectively (Figure 2). Trp724 and Trp652 contributed approximately 70% and 30%, respectively, to the total Trp fluorescence of Div protein under these conditions. These spectral properties are similar to those inferred for the corresponding residues of *E. coli* SecA protein (*58*, *59*).

The C-terminus of SecA and the Cys residues contained therein have been shown to be dispensable for SecA function

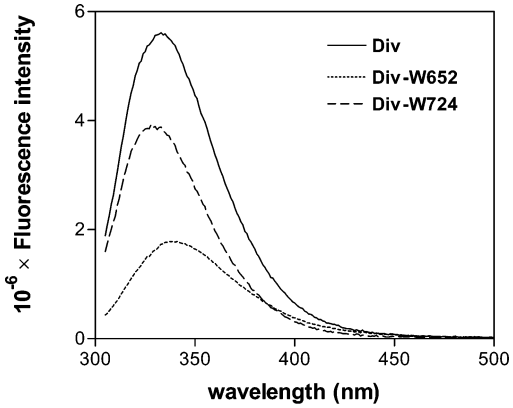

FIGURE 2: Fluorescence emission spectra of Div proteins. Fluorescence spectra of Div protein at 40 μg/mL in TKE buffer was collected at 24 °C using an excitation wavelength of 297 nm.

(*60*, *61*). Accordingly, genetic engineering methodology was used to change the four Cys residues present within this region to Ser or His, resulting in Div-C4 protein that lacks any cysteine. This protein was then further modified genetically by changing one of the two Trp residues to Phe as well as introducing unique Cys residues at appropriate positions within the SecA structure (Figure 1A). Thus, we generated SecA proteins that contain unique Trp and Cys pairs for conducting FRET studies to investigate SecA oligomeric structure.

During purification of these mutant proteins on SP-Sepharose and hexyl agarose, we noted that they had elution profiles that were similar to wild-type Div protein. Furthermore, their secondary structure was similar to wild-type Div based on their CD spectra (data not shown). In addition, each mono-Trp mono-Cys mutant protein had a fluorescence profile that was similar to that of its mono-Trp parent protein, either Div-W652 or Div-W724 (data not shown), indicating that the Trp environments were relatively unperturbed by the Cys mutations.

To investigate the biochemical activity of these mutant proteins, ATPase assays were performed. SecA protein possesses three distinct ATPase activities: an endogenous ATPase activity in solution, a SecYEG-stimulated ATPase activity (termed membrane ATPase), and a preprotein and SecYEG-stimulated ATPase activity (termed translocation ATPase). We found that all of the mutant proteins possessed the three different SecA dependent ATPase activities, although there was some variation in the amount of a given activity depending on the particular mutant protein (Figure 3). All of the observed translocation ATPase activities should be well within the range required for good protein translocation activity (*51*, *62*). Importantly, we noted that the membrane and translocation ATPase activities of Div and most of its derivatives were completely dependent on the presence of *B. subtilis* SecYEG protein in the IMV preparations utilized. IMV containing solely *E. coli* SecYEG protein was generally inactive in stimulating these latter two ATPase activities, consistent with the inability of *B. subtilis* and *E. coli* SecA proteins to function in vivo and in vitro across this species barrier (*50*, *63*). The requirement of Div for its homologous SecYEG complex for functionality has been demonstrated previously (*53*). Certain exceptions to this pattern were noted, however. For example, Div-W724−C6 protein had a high level of membrane ATPase activity in the presence of either *B. subtilis* or *E. coli* SecYEG protein. In this latter case, however, IMV containing solely *E. coli* SecYEG protein elicited a negative translocation ATPase activity (i.e., inhibited the ATPase activity). This result suggests that in certain cases the presence of particular substitutions within Div may allow it to interact favorably with *E. coli* SecYEG protein, even though such interaction may not lead to a productive overall protein translocation cycle. Mutations within SecA and SecY that enhance the interaction of these two proteins have been observed previously including ones that lead to nonproductive translocation and translocation ATPase activities (*64*−*67*). On the basis of our structural and biochemical characterization of these mutant proteins, we concluded that they were suitable for MIANS labeling and FRET analysis.

MIANS Labeling of SecA Proteins. We chose to utilize the sulfhydryl-labeling fluorophore MIANS for our study since the absorption peak of its SH-conjugated adduct at approximately 324 nm displayed good spectral overlap with the fluorescence maximum of Trp724 and Trp652 of Div at 330 and 339 nm, respectively (Figure 4). We found that the

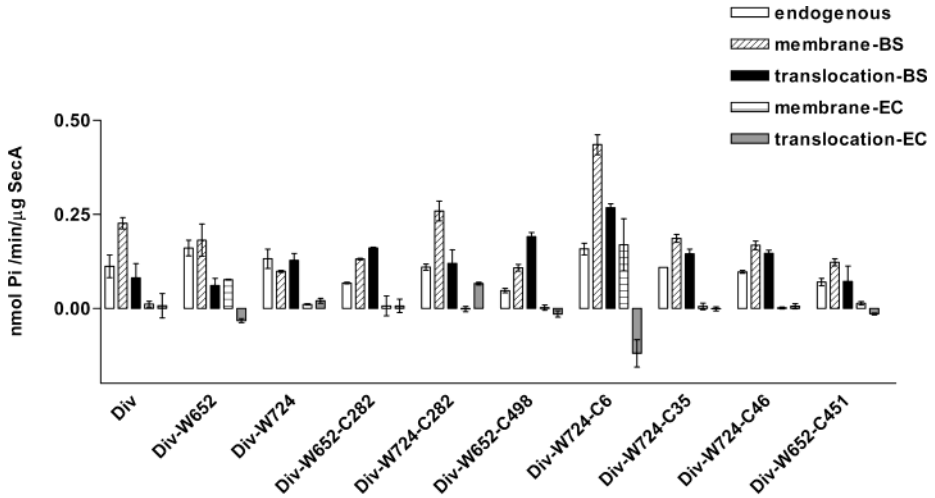

FIGURE 3: ATPase activities of mutant Div proteins. Endogenous, membrane, and translocation ATPase activity of each mutant Div protein is indicated. EC and BS indicate assays with IMV prepared from SF100 producing solely *E. coli* SecYEG and SF100 (pET822) overproducing *B. subtilis* SecYEG, respectively. Duplicate assays were performed, and the standard deviation is indicated.

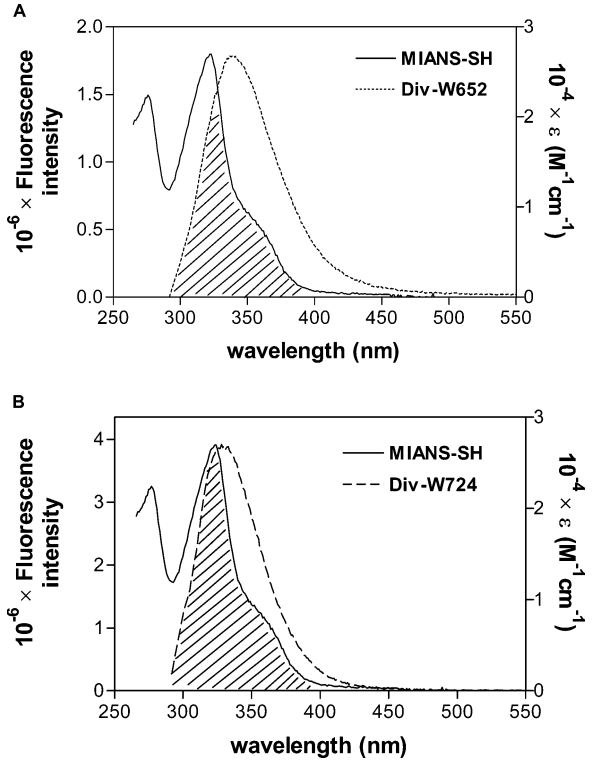

FIGURE 4: Overlap of the Trp fluorescence emission spectrum of Div protein with the absorption spectrum of MIANS-SH. (A) Div-W652 protein and MIANS-SH; (B) Div-W724 protein and MIANS-SH. Spectra for Div proteins were collected as described in the Figure 1 legend. Absorption of MIANS-SH in TKE buffer was collected at room temperature from 250 to 550 nm.

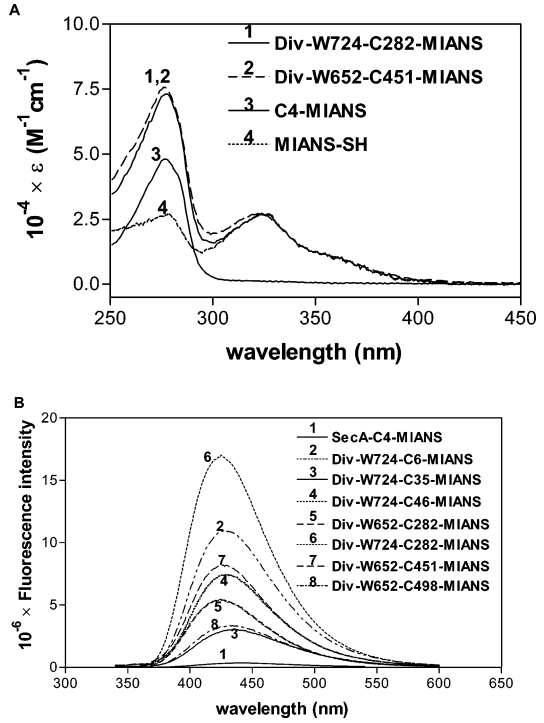

FIGURE 5: Spectra of MIANS-labeled Div proteins. (A) Absorption and (B) fluorescence emission spectra of MIANS-labeled Div proteins. The experimental conditions for panels A and B were identical to those described in the Figure 4 and Figure 1 legends, respectively, with the exception that an excitation wavelength of 324 nm was used for panel B and the data were normalized to 100% labeling efficiency.

absorption maximum of the SH adduct was essentially identical to that observed for the different MIANS-labeled SecA proteins (Figure 5, panel A; and data not shown). On the basis of the spectral overlap, we calculated Förster distances for MIANS-SH and Div-W652 or Div-W724 (see Experimental Procedures).

MIANS labeling conditions were found that resulted in nearly quantitative labeling of the mutant SecA proteins (>90%) (see Experimental Procedures). To check the specificity of our labeling procedure, we utilized Div-C4 protein that does not have any cysteine residues as a negative control. Div-C4 protein was not labeled by MIANS under our experimental conditions based upon the absence of absorption at 324 nm (Figure 5, panel A). It should be noted that MIANS is not fluorescent until it is conjugated to a sulfhydryl group (*68*), and this was true for the labeled proteins used in this study as well. Furthermore we found that the fluorescence spectrum was generally unique to the particular MIANS-labeled SecA protein, indicative of a Cys-specific labeling pattern that was environmentally sensitive (Figure 5, panel B). Certain inferences could be made about the local environment of the particular MIANS-labeled residue based on these spectra. Examination of MIANS-SH in different solvents revealed that the fluorescence maximum shifts to the blue in nonpolar solvents ((*69*); also results not shown). Therefore, the emission maxima of Cys6, Cys46, Cys282, and Cys451 that occur at 429, 429, 425, and 427 nm, respectively, are indicative of a more local hydrophobic environment, while that of Cys35 and Cys498 at 436 and 434 nm, respectively, appear to be in a more hydrophilic environment based on this criterion. We cannot rule out the possibility, however, that the Cys substitution and MIANS label may contribute to the observed results.

To evaluate the biochemical activity of the MIANS-labeled SecA proteins, ATPase assays were performed. We found that the MIANS-labeled SecA proteins had endogenous, membrane, and translocation ATPase activities that were essentially identical to their non-MIANS-labeled counterparts (data not shown). This latter result indicates that the MIANS label did not perturb the function of the particular SecA proteins under study.

FRET Analysis of MIANS Labeled SecA Proteins. FRET experiments were performed to determine the oligomeric architecture of SecA. The results of our analysis are summarized in Table 1, and several representative experiments are shown in Figure 6. A decrease in Trp fluorescence emission intensity in the presence of the MIANS label was indicative of energy transfer. Such a decrease was observed for all pairs except W724−C35, indicating that the interfluorophore separation was >56 Å in this latter case. For all of the other pairs, the interfluorophore distances were calculated based on the quenching of donor fluorescence using eqs 1 and 2. The data were grouped into Trp−Cys pairs that gave intraprotomer or interprotomer FRET based on the agreement between the distances inferred from the crystal structure of Div and what was experimentally determined by FRET.

In the case of the Trp652−Cys282, Trp724−Cys46, and Trp724−Cys282 pairs, there was good agreement between the protomer distances measured from the crystal structure of Div and the experimentally determined values from FRET (Table 1; Figure 6, panel A). Several factors would be

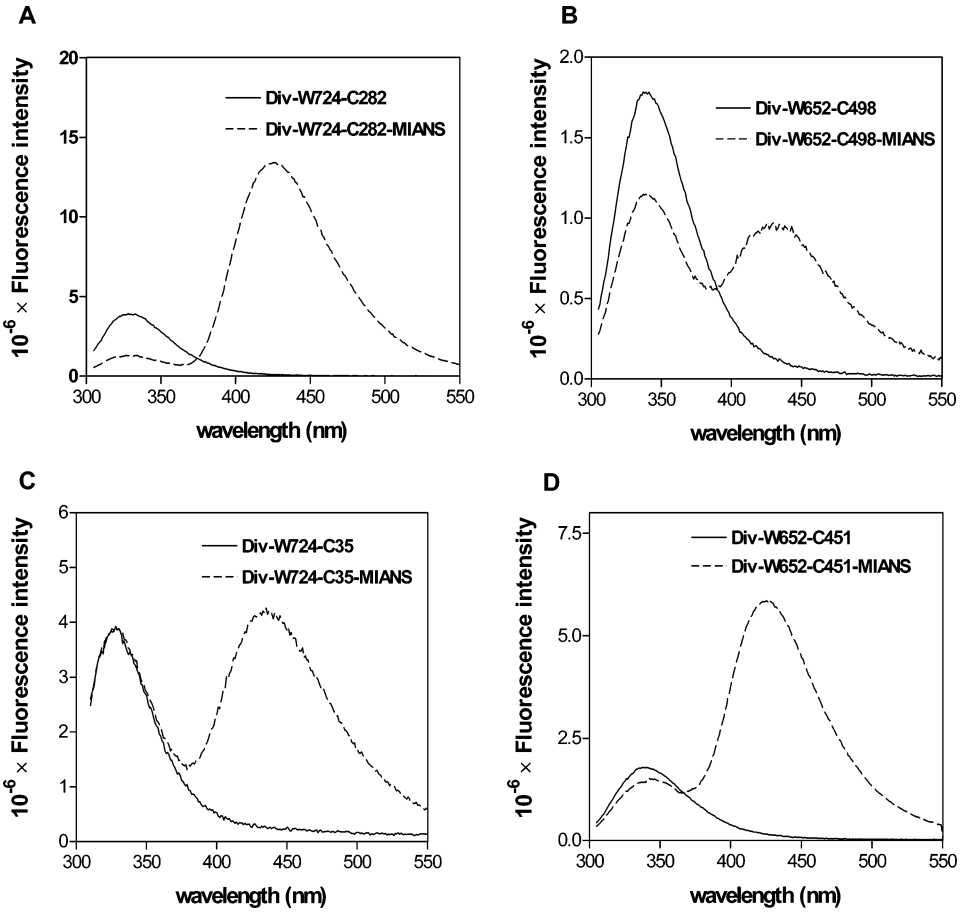

FIGURE 6: FRET analysis of mutant Div proteins. The fluorescence emission spectra of MIANS-labeled and unlabeled Div proteins were compared. (A) Div-W724−C282, (B) Div-W652−C498, (C) Div-W724−C35, and (D) Div-W652−C451. All fluorescence emission spectra were measured at 40 μg/mL Div protein in TKE buffer at 24 °C using an excitation wavelength of 297 nm.

Table 1: FRET Results and Inter-Residue Distances in Potential *B. subtilis* SecA Oligomers[a]

		distance measurements (Å)				
Trp site	Cys site	FRET[b]	intra-protomer	antiparallel dimer	alternative dimer	3_1 fiber[c]
		Site Pairs Giving Intraprotomer FRET				
652	282	35 ± 1	36	89	100	60, 80, 87, 155
724	46	45 ± 5[d]	46	59	27	99, 107, 124, 129
724	282	26 ± 1	20	76	75	67, 67, 93, 139
		Site Pairs Giving Interprotomer FRET				
652	451	34 ± 2[e]	92	39	141	17, 98, 112, 126
652	498	24 ± 2	96	33	88	36, 105, 124, 147
724	6	28 ± 2	53	17	70	68, 87, 90, 127
		Site Pair Giving No FRET				
724	35	>56[d]	60	60	29	99, 118, 122, 140

[a] Distances were measured between the Cα atoms of the residues in the crystal structure of *B. subtilis* SecA (27) using the program O (73). [b] Mean values and standard deviations are given for the interfluorophore distances calculated from three FRET experiments (see Experimental Procedures). [c] This structure represents the packing of antiparallel dimers into a helix with 3_1 symmetry, which gives four new unique interfluorophore distances upon formation. [d] FRET measurements excluding the alternative dimer. [e] FRET measurement excluding 3_1 fiber formation.

expected to contribute to minor discrepancies between these two numbers. First, our predicted distances were based on the separation between the Cα atoms of the donor and acceptor residues because the uncertainty in the interfluorophore distance introduced by the dihedral flexibility of the MIANS label makes more detailed calculations unrealistic. Second, our calculations assumed a randomly oriented donor and acceptor pair (see Experimental Procedures), which may not always be the case, given possible orientation biases of the probes within certain local environments. However,

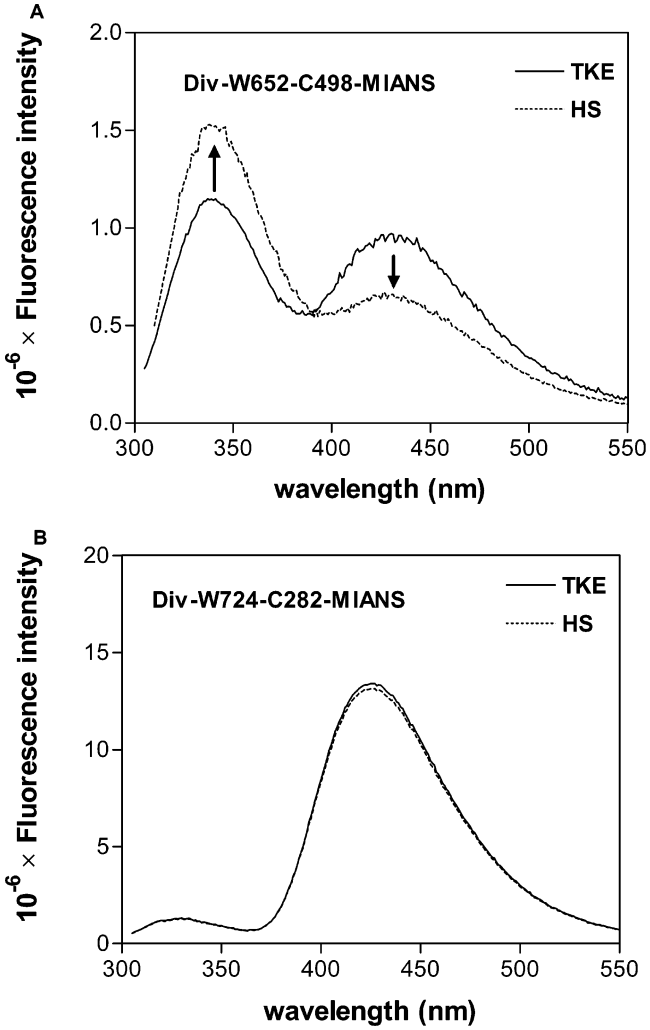

FIGURE 7: Effect of high salt concentration on FRET of Div proteins. The fluorescence emission spectra of MIANS-labeled Div proteins in TKE buffer (TKE) or buffer containing 300 mM KCl (HS) were compared. (A) Div-W652−C498-MIANS and (B) Div-W724−C282-MIANS. The fluorescence emission spectra were collected at 40 μg/mL Div protein in the indicated buffer at 24 °C using an excitation wavelength of 297 nm. Upward and downward arrows indicate increased Trp fluorescence and decreased MIANS fluorescence, respectively.

Trp654 and Trp724 are located in relatively mobile regions of Div as inferred from atomic B-factors of the refined crystal structure of the protein (*27*).

The results obtained for the Trp652−Cys451, Trp652−Cys498, and Trp724−Cys6 pairs were consistent with the antiparallel dimer (Table 1; Figure 1, panels B and C; Figure 6, panel B). The 11 Å difference between the predicted and observed distances for the Trp724−Cys6 pair may be due to the mobility of the amino-terminus of Div protein in solution. The FRET measurements on the Trp724−Cys35 and Trp724−Cys46 pairs directly tested the occurrence of the alternative dimer, and the results from these pairs provided no support for its existence (Table 1; Figure 6, panel C). FRET should have been highly efficient for both pairs but was not found to be so in this case. From these results we conclude that the antiparallel dimer is the correct structure for SecA dimer in solution.

Finally, the Trp652−Cys451 pair enabled the formation of higher-order Div oligomers with 3_1 helical symmetry to be monitored (see Introduction). The measured FRET efficiency for this site pair argues against formation of 3_1 helical fiber interactions under the low protein concentration conditions used in these experiments (Table 1). A 17 Å difference was observed between the experimentally inferred distance and that predicted to occur in the 3_1 helical fiber. In this case, contrary to the W724−C6 pair, the Trp and Cys residues are expected to be in relatively static regions of the protein and therefore, a large discrepancy between predicted and observed distances is unlikely. Furthermore, we saw no evidence for the occurrence of this 3_1 helical fiber interaction (in the form of concentration dependent changes in FRET efficiency) even when the Div protein concentration was increased by 5-fold (data not shown). Higher concentrations of Div protein could not be evaluated using our FRET system due to the inner filter effect.

A recent study indicated that SecA has a monomer−dimer equilibrium in the micromolar range that is quite sensitive to salt concentration (*21*). At the salt concentration employed in our studies, most SecA proteins should be present in the dimeric form. However, to experimentally address this point, we compared the fluorescence spectra of an appropriately chosen Div protein under our buffer conditions with that of Woodbury et al., who included 300 mM KCl in their standard assay conditions (*21*). It is clear that inclusion of physiological salt resulted in a decrease of FRET for Div-W652−C498-MIANS, consistent with the monomerization of a significant fraction of this protein (Figure 7A). A similar experiment conducted on a protein that contained a Trp−Cys pair that reported only on protomer distance, Div-W724−C282-MAINS, indicated that the change in salt had no effect on the observed fluorescence spectrum (Figure 7B). These results confirm those of Woodbury et al. and indicate that our studies were conducted under conditions that were sensitive for detecting SecA oligomers. In addition, they indicate that FRET is a useful method for assessing the oligomeric state of SecA under various experimental conditions.

DISCUSSION

SecA ATPase is an unusually complex, multidomain protein that has interactions with most of the components of the secretion pathway. These interactions, along with the nucleotide binding and hydrolytic cycle of SecA, drive conformational changes within SecA that trigger its membrane cycling and promote the protein translocation cycle (*17*, *18*). SecA has been shown to have a more compact, ADP-bound state in solution that undergoes a major conformational change to a more extended state after binding to membranes containing anionic phospholipids (*27*, *58*, *70*). ATP analogues also induce a more extended conformation of SecA that may be similar to its membrane-bound state (*58*). The structures of phospholipid and translocon-bound SecA, as well as those changes that are induced by ATP and preprotein binding and which lead to SecA membrane cycling, are not known.

In the present study, we have defined the subunit orientation and stoichiometry of SecA protein in solution. The FRET measurements indicate that the antiparallel dimer identified in our report of the crystal structure of SecA (*27*) is present in solution and that neither of the other oligomeric interfaces observed in the crystal tend to form, at least at the low protein

concentrations used in these studies. Our identification of the structure of the SecA dimer in solution state is consistent with a report that the C-terminal third of SecA protein mediates its dimerization (*71*). It is also consistent with the recent crystal structure of SecA protein from *M. tuberculosis* that appeared during review of our work, which also contains antiparallel dimers that associate into a tetramer (*23*).

Beyond establishing the geometry of the SecA dimer in solution state, these studies provide a starting point for future studies aimed at defining the structural dynamics of SecA at different points in the protein translocation cycle. Our FRET study with appropriately designed Trp and fluorophore-labeled Cys resides points out the feasibility of this approach, where different domain-domain interactions of SecA and their dynamics in the presence of various translocation ligands can now be reasonably assessed. Such studies should be pivotal for understanding the mechanics of the SecA motor as well as the thermodynamics of the protein translocation cycle.

Our studies assume unusual relevance given recent reports describing the monomer−dimer equilibrium of SecA in solution as well as the apparently dramatic effects that translocation ligands can have on this equilibrium (*21*, *25*, *26*). Our data are consistent with those of Woodbury et al, who found that the monomer−dimer equilibrium of SecA is sensitive to both temperature and salt concentration (*21*). At the temperature and salt concentration employed in our study, most SecA protein should be in the dimer form similar to the study of Doyle et al. (*72*). However, we noted that a shift of SecA from dimeric to monomeric form could be induced when 300 mM KCl was included in our assay conditions, as previously observed (*21*). These collective observations indicate that the SecA monomer−dimer transition is sensitive to modulation by various factors, and this feature may play a significant role in SecA function during protein translocation.

A recent report has suggested that SecA is active as a monomer based on the ability of anionic phospholipids and SecYE protein binding to induce SecA monomerization as well as the fact that a largely monomeric mutant of SecA retained some residual in vitro protein translocation activity despite a severe impairment in its functionality (*25*). This report contradicts an earlier one indicating that SecA is active as a dimer (*24*). While the FRET approach utilized in this latter study to assess SecA subunit status may not have been sensitive enough to detect a lesser albeit important fraction of SecA monomer in the membrane, the observed inactivity of SecA heterodimers comprised of wild-type and 8-azido-ATP-inactivated subunits is difficult to reconcile unless SecA functions as a dimer at some stage in the protein translocation cycle. Further complicating this picture is the report from one of our laboratories that interaction of SecA protein with signal peptides in the presence of anionic phospholipids was sufficient to restore dimer formation (*26*). Clearly, additional studies will be needed to obtain a better understanding of the subunit status, oligomeric structure, and dynamics of SecA during its interactions with its various partners during protein translocation. Our present study, which defines the dominant species of SecA in solution as the antiparallel dimer, sets the stage for this important task.

ACKNOWLEDGMENT

We thank Chris Zito for IMV preparation and Kristi Poulin for help with the spectroscopy and data analysis.

REFERENCES

1. Manting, E. H., and Driessen, A. J. M. (2000) *Mol. Microbiol. 37*, 226−238.
2. Mori, H., and Ito, K. (2001) *Trends Microbiol. 9*, 494−500.
3. Beck, K., Wu, L.-F., Brunner, J., and Muller, M. (2000) *EMBO J. 19*, 134−143.
4. Koch, H.-G., Hengelage, T., Neumann-Haefelin, C., MacFarlane, J., Hoffschulte, H., Schimz, K.-L., Mechler, B., and Muller, M. (1999) *Mol. Biol. Cell 10*, 2163−2173.
5. Qi, H.-Y., and Bernstein, H. (1999) *J. Biol. Chem. 274*, 8993−8997.
6. Scotti, P., Valent, Q., Manting, E., Urbanus, M., Driessen, A., Oudega, B., and Luirink, J. (1999) *J. Biol. Chem. 274*, 29883−29888.
7. Tian, H., Boyd, D., and Beckwith, J. (2000) *Proc. Natl. Acad. Sci. U.S.A. 97*, 4730−4735.
8. Samuelson, J. C., Chen, M., Jiang, F., Moller, I., Wiedmann, M., Kuhn, A., Phillips, G., and Dalbey, R. (2000) *Nature 406*, 637−641.
9. Scotti, P. A., Urbanus, M. L., Brunner, J., de Gier, J.-W., von Heijne, G., van der Does, C., Driessen, A., Oudega, B., and Luirink, J. (2000) *EMBO J. 19*, 542−549.
10. Meyer, T., Menetret, J.-F., Breitling, R., Miller, K., Akey, C., and Rapoport, T. (1999) *J. Mol. Biol. 285*, 1789−1800.
11. Manting, E. H., van der Does, C., Remigy, H., Engel, A., and Driessen, A. J. M. (2000) *EMBO J. 19*, 852−861.
12. Collinson, I., Breyton, C., Duong, F., Tziatzios, C., Schubert, D., Or, E., Rapoport, T., and Kuhlbrandt, W. (2001) *EMBO J. 20*, 2462−2471.
13. Nishiyama, K.-I., Suzuki, T., and Tokuda, H. (1996) *Cell 85*, 71−81.
14. Duong, F., and Wickner, W. (1997) *EMBO J. 16*, 4871−4879.
15. Nouwen, N., and Driessen, A. (2002) *Mol. Microbiol. 44*, 1397−1405.
16. Pohlschroder, M., Prinz, W. A., Hartmann, E., and Beckwith, J. (1997) *Cell 91*, 563−566.
17. Economou, A., and Wickner, W. (1994) *Cell 78*, 835−843
18. van der Wolk, J. P. W., de Wit, J. G., and Driessen, A. J. M. (1997) *EMBO J. 16*, 7297−7304.
19. Chen, X., Xu, H., and Tai, P. (1996) *J. Biol. Chem. 271*, 29698−29706
20. Shilton, B., Svergun, D. I., Volkov, V. V., Koch, M. H., Cusack, S., and Economou, A. (1998) *FEBS Lett. 436*, 277−282.
21. Woodbury, R. L., Hardy, S., and Randall, L. (2002) *Protein Sci. 11*, 875−882.
22. Weinkauf, S., Hunt, J. F., Scheuring, J., Henry, L., Fak, J., Oliver, D. B., and Deisenhofer, J. (2001) *Acta Crystallogr. D57*, 559−565.
23. Sharma, V., Arockiasamy, A., Ronning, D. R., Savva, C. G., Holzenburg, A., Braunstein, M., Jacobs, W. R., and Sacchettini, J. C. (2003) *Proc. Natl. Acad. Sci. U.S.A. 100*, 2243−2248.
24. Driessen, A. (1993) *Biochemistry 32*, 13190−13197.
25. Or, E., Navon, A., and Rapoport, T. (2002) *EMBO J. 21*, 4470−4479.
26. Benach, J., Chou, Y.-T., Fak, J. J., Itkin, A., Nicolae, D. D., Smith, P. C., Wittrock, G., Floyd, D. L., Golsaz, C. M., Gierasch, L. M., and Hunt, J. F. (2002) *J. Biol. Chem. 278*, 3628−3638.
27. Hunt, J. F., Weinkauf, S., Henry, L., Fak, J. J., McNicholas, P., Oliver, D. B., and Deisenhofer, J. (2002) *Science 297*, 2018−2026.
28. Schmidt, M. G., Rollo, E. E., Grodberg, J., and Oliver, D. B. (1988) *J. Bacteriol. 170*, 3404−3414.
29. Sadaie, Y., Takamatsu, H., Nakamura, K., and Yamane, K. (1991) *Gene 98*, 101−105.
30. Chakrabarti, P., and Janin, J. (2002) *Proteins 47*, 334−343.
31. Ponstingl, H., Henrick, K., and Thornton, J. M. (2000) *Proteins 41*, 47−57.
32. Janin, J. (1997) *Nat. Struct. Biol. 4*, 973−974.
33. Dasgupta, S., Iyer, G. H., Bryant, S. H., Lawrence, C. E., and Bell, J. A. (1997) *Proteins 28*, 494−514.
34. Janin, J., and Rodier, F. (1995) *Proteins 23*, 580−587.

35. Janin, J., and Chothia, C. (1990) *J. Biol. Chem. 265*, 16027−16030.
36. Janin, J., Miller, S., and Chothia, C. (1988) *J. Mol. Biol. 204*, 155−164.
37. Miller, S., Lesk, A. M., Janin, J., and Chothia, C. (1987) *Nature 328*, 834−836.
38. Diederichs, K., Diez, J., Greller, G., Muller, C., Breed, J., Schnell, C., Vonrhein, C., Boos, W., and Welte, W. (2000) *EMBO J. 19*, 5951−5961.
39. Yuan, Y. R., Blecker, S., Martsinkevish, O., Millen, L., Thomas, P. J., and Hunt, J. F. (2001) *J. Biol. Chem. 276*, 32313−32321.
40. Smith, P. C., Firestein, S., and Hunt, J. F. (2002) *J. Mol. Biol. 319*, 807−821.
41. Lakowicz, J. R. (1999) in *Principles of Fluorescence Spectroscopy*, 2nd ed., pp 367−394, Plenum Publishers, New York.
42. Beechem, J. M. (1997) *Methods Enzymol. 278*, 24−49.
43. Lillo, M. P., Beechem, J. M., Szpikowska, B. K., Sherman, M. A., and Mas, M. T. (1997) *Biochemistry 36*, 11261−11272.
44. Lillo, M. P., Szpikowska, B. K., Mas, M. T., Sutin, J. D., and Beechem, J. M. (1997) *Biochemistry 36*, 11273−11281.
45. Hillisch, A., Lorenz, M., and Diekmann, S. (2001) *Curr. Opini. Struct. Biol. 11*, 201−207.
46. Cheung, H. C. (1991) in *Topics in Fluorescence Spectroscopy* (Lakowicz, J. R., Ed) Vol. 2, pp 127−176, Plenum, New York.
47. Heyduk, T. (2002) *Curr. Opin. Biotechnol. 13*, 292−296.
48. Dong, W. J., Xing, J., Robinson, J. M., and Cheung, H. C. (2001) *J. Mol. Biol. 314*, 51−61.
49. Trakselis, M. A., Alley, S. C., Abel-Santos, E., and Benkovic, S. J. (2001) *Proc. Natl. Acad. Sci. U.S.A. 98*, 8368−8375.
50. McNicholas, P., Rajapandi, T., and Oliver, D. (1995) *J. Bacteriol. 177*, 7231−7237.
51. Mitchell, C., and Oliver, D. B. (1993) *Mol. Microbiol. 10*, 483−497.
52. Lanzetta, P. A., Alvarez, L. J., Reinach, P. S., and Candia, O. A. (1979) *Anal. Biochem. 100*, 95−97.
53. Swaving, J., van Wely, K., and Driessen, A. (1999) *J. Bacteriol. 181*, 7021−7027.
54. Dapic, V., and Oliver, D. (2000) *J. Biol. Chem. 275*, 25000−25007.
55. Cabelli, R. J. (1991) *Biochemical Characterization of the Role of SecA Protein in Protein Export in Escherichia coli*, State University of New York, Stony Brook, NY.
56. Chen, R. F. (1967) *Anal. Lett. 1*, 35−42.
57. Weber, G., and Shinitzky, M. (1970) *Proc. Natl. Acad. Sci. U.S.A. 65*, 823−830.
58. den Blaauwen, T., Fekkes, P., de Wit, J. G., Kuiper, W., and Driessen, A. J. M. (1996) *Biochemistry 35*, 11994−12004.
59. Ding, H., Mukerji, I., and Oliver, D. (2001) *Biochemistry 40*, 1835−1843.
60. Rajapandi, T., and Oliver, D. (1994) *Biochem. Biophys. Res. Commun. 200*, 1477−2483.
61. Matsuyama, S., Kimura, E., and Mizushima, S. (1990) *J. Biol. Chem. 265*, 8760−8765.
62. Kourtz, L., and Oliver, D. (2000) *Mol. Microbiol. 37*, 1342−1356.
63. Takamatsu, H., Fuma, S.-I., Nakamura, K., Sadaie, Y., Shinkai, A., Matsuyama, S.-I., Mizushima, S., and Yamane, K. (1992) *J. Bacteriol. 174*, 4308−4316.
64. van der Wolk, J., Fekkes, P., Boorsma, A., Huie, J., Silhavy, T., and Driessen, A. (1998) *EMBO J. 17*, 3631−3639.
65. Matsumoto, G., Yoshihisa, T., and Ito, K. (1997) *EMBO J. 16*, 6384−6393.
66. Nakatogawa, H., Mori, H., Matsumoto, G., and Ito, K. (2000) *J. Biochem. 127*, 1071−1079.
67. Manting, E., Kaufmann, A., van der Does, C., and Driessen, A. (1999) *J. Biol. Chem. 274*, 23868−23874.
68. Haugland, R. P. (1996) *Handbook of Fluorescent Probes and Research Chemicals*, 6th ed., Molecular Probes, Inc., Eugene, OR.
69. Hiratsuka, T. (1992) *J. Biol. Chem. 267*, 14941−14948.
70. Ulbrandt, N. D., London, E., and Oliver, D. B. (1992) *J. Biol. Chem. 267*, 15184−15192.
71. Hirano, M., Matsuyama, S., and Tokuda, H. (1996) *Biochem. Biophys. Res. Commun. 229*, 90−95.
72. Doyle, S. M., Braswell, E. H., and Teschke, C. M. (2000) *Biochemistry 39*, 11667−11676.
73. Jones, T. A., Zou, J.-Y., Cowan, S. W., and Kjeldgaard, M. (1991) *Acta Crystallogr. A47*, 110−119.
74. Kraulis, P. J. (1991) *J. Appl. Crystallogr. 24*, 946−950.
75. Merritt, E. A., and Bacon, D. J. (1997) *Methods Enzymol. 277*, 505−524.

BI0342057